A Possible Mechanism for Controlling Timing Representation in the Cerebellar Cortex

Takeru Honda[1,2], Tadashi Yamazaki[3], Shigeru Tanaka[1,2], and Tetsuro Nishino[1]

[1] Faculty of Electro-Communications, The University of Electro-Communications, 1-5-1 Chofugaoka, Chofu-shi, Tokyo 182-8585, Japan
[2] RIKEN Brain Science Institute, 2-1 Hirosawa, Wako-shi, Saitama 351-0198, Japan
[3] RIKEN BSI-TOYOTA Collaboration Center, 2-1 Hirosawa, Wako-shi, Saitama 351-0198, Japan
{takeru,shigeru,nishino}@ice.uec.ac.jp, tyam@brain.riken.jp

Abstract. We have developed a network model of cerebellar cortex, in which granular cells' activities represent a passage of time from the onset of a conditioned stimulus (CS). Long-term depression of parallel fiber synapses at Purkinje cells (PCs) encodes an interstimulus interval between onsets of a CS and an unconditioned stimulus (US) as cessation of PC firing, resulting in the emission of a conditioned response (CR) from cerebellar nucleus neurons. In this study, we show that a change in the strength of a CS extends or compresses spike trains of granule cells in the time dimension, suggesting controllability of CR timings flexibly after conditioning. Because PCs alone are insufficient to read out a modified interstimulus interval, we add stellate cells (SCs) inhibiting PCs. Thereby, after conditioning, PCs are shown to stop firing earlier or later than the US timing for a CS stronger or weaker than the CS during conditioning.

Keywords: Cerebellum, Spiking network model, Passage of time, Eyeblink conditioning, Adaptive timing.

1 Introduction

The cerebellum is widely accepted to control the performance of motor actions precisely [1]. Achievement of temporally coordinated motor actions requires precise timing of each action. Very recently, we have proposed that neural dynamics of the granular layer in the cerebellar cortex represents the passage of time (POT) from the onset of a sustained conditioned stimulus (CS) conveyed by mossy fibers (MFs) as a temporal sequence of active granule cell (GRC) populations [2]. Combining with long-term depression (LTD) at synaptic junctions of parallel fibers (PFs) from GRCs to PCs, which is induced by repetitive pairings with a CS and an unconditioned stimulus (US) conveyed by the climbing fibers, PCs stop firing at the timing of the US presented during conditioning. The cessation of the PC firing releases tonic inhibition to cerebellar nucleus neurons that receive direct MF signals, and elicits a conditioned response (CR) as the nucleus neurons' activation.

When we apply these computational mechanisms to the conditioning of motor reflex, it can be accounted for the temporal topography of a CR to a CS presentation.

L. Zhang, J. Kwok, and B.-L. Lu (Eds.): ISNN 2010, Part I, LNCS 6063, pp. 67–76, 2010.

A typical example of such conditioning is Pavlovian delay eyeblink conditioning (for review, e.g., [3], [4], [5], [6]). Particularly, in this conditioning, a subject is exposed to paired presentation of a sustained tone as a CS and an airpuff as a US that induces eyeblink reflex. After the repeated conditioning by CS-US presentation with a fixed interstimulus interval (ISI) between the CS and US onsets, the CS presentation alone let the subject close the eye as a CR slightly prior to the US onset timing.

In our simulations of a conditioned cerebellar network, we found that spike trains elicited by GRCs were extended or compressed for a CS stronger or weaker than the CS during the conditioning, which indicates that a stronger CS let a POT shorter whereas a weaker CS let it longer. This possibility is suggested by a recent experiment, in which a CR was elicited earlier when the strength of a tonal stimulus (CS) was increased. However, in the simulations, when we changed the strength of a CS, a model PC did not stop firing clearly. This suggests that the PC's read-out mechanism of a POT represented by GRCs is not sufficient. In the present study, we incorporate a stellate cell (SC) that inhibits the PC. We assumed that the model SC receives climbing fiber inputs and CS-US conjunctive stimulation induces long-term potentiation (LTP). Simulations showed that the model PC successfully stop firing earlier or later than the timing of a CR elicited by the CS presented during conditioning. It is suggested that SCs work to assist and enhance the PC's read-out mechanism of a POT.

2 Methods

We build our model based on the GENESIS script of the granular layer model, which was written by Maex and De Schutter [7]. Briefly, we extend the original one-dimensional network structure to two-dimensional one and set random connections from model Golgi cells (GOCs) to GRCs (Fig. 1). We also extend their single-compartment GOC model to a multi-compartment model composed of a soma and a dendrite, on which voltage-gated *N*-methyl-*D*-aspartate (NMDA) channels are distributed. We change values of some model parameters so that the network behaves stably.

2.1 Network Structure

In the present model, 32×32 model GOCs are arranged in two-dimensional grids (Fig. 1), in which the model GOCs are evenly positioned at 35 μm intervals within the square sheet of 1,085×1,085 μm^2. It was estimated that there were 1000 times more GRCs than GOCs [8]. Numerous GRCs were connected with a glomerulus [9]. However, simulation with more than 1 million model neurons is beyond the power of our computers. In Yamazaki and Tanaka [10], 100 nearby GRCs that were assumed to be connected with a glomerulus exhibited similar firing patterns despite each of the GRCs received noisy signals through MFs independently. Such redundant activity patterns of GRCs suggest that many GRCs behave as a single cluster when they receive inputs from a nearest GOC through a single glomerulus. In the present model, for the sake of the economy of computer power, we assume that a single model GRC represents a GRC cluster composed of about 1,000 neurons (Fig. 1).

We assume that a GOC receives 9×32 PF inputs from model GRCs with its dendritic arborization whose diameter is set at 315 μm, and the connection probability

of a PF at the GOC is set at 0.1. The model GOC, in turn, sends inhibitory inputs to model GRCs located within the extent of axonal arborization, which is set at 315 μm, so that a model GRC receives inhibitory inputs from 69 nearby model GOCs (Fig. 1). The connection probability from a GOCs to a model GRCs is set at 0.1.

The model network contains 1 PC and 1 SC (Fig. 2). The model PC and SC receive PF inputs from GRCs and climbing fiber inputs that convey US signals. The SC sends an inhibitory connection to the PC.

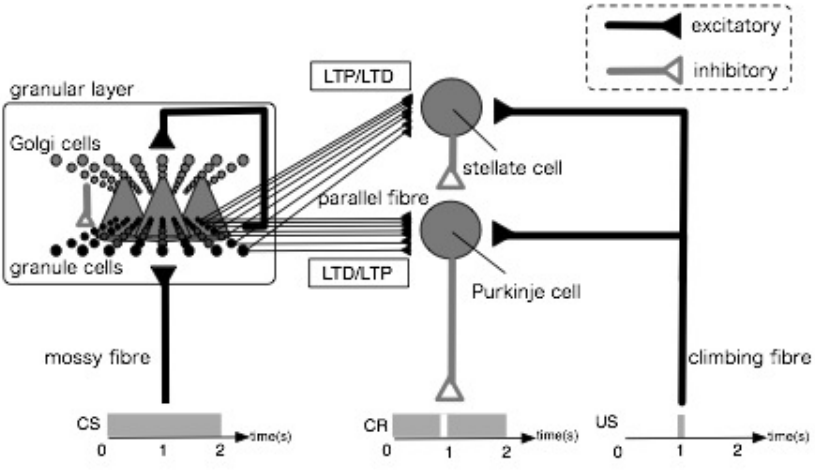

Fig. 1. A schematic of the cerebellar network model. GOCs receive excitatory inputs from GRCs and recurrently inhibit GRCs. Thus, GRCs and GOCs construct a recurrent inhibitory network. Grcs receive CS signals and, in turn, excite a PC and an SC. Paring of US signals fed to a PC and SC with CS signals induce LTD and LTP at PF terminals at these cells.

2.2 Granule and Golgi Cell Models

We use a model GRC composed of a single-compartment Hodgkin-Huxley unit, as adopted by Maex and De Schutter [7]. We simulate inhibitory postsynaptic potential (IPSP) induced by γ-aminobutyric acid type A ($GABA_A$) receptor/channels using a double-exponential function with rise and decay time constants of 5 ms and 100 ms, respectively.

On the other hand, a GOC is modeled as a multi-compartment Hodgkin-Huxley unit composed of a soma and a dendrite, rather than a single-compartment unit as in Maex and De Schutter [7]. The model GOCs receive excitatory inputs from model GRCs through α-amino-3-hydroxy-5-methyl-4-isoxazolepropionic acid (AMPA) channels with rise and decay time constants of 0.03 ms and 0.5 ms, respectively.

It has been found that GOCs receive excitatory input signals from PFs through not only AMPA but also NMDA channels [11]. However, even when we add NMDA channels at the somas of model GOCs, the NMDA channels do not open effectively to evoke sustained depolarization because after-hyperpolarization (AHP) [12][13] following each action potential generation rapidly decreases somatic membrane

potential. On the other hand, it is known that the dendritic potential tends not to be affected by AHP at cell somas [12]. Moreover, it has been shown that direct dendritic excitation produces sustained and burst responses although somatic excitation does not [12]. If NMDA channels really function to induce a prolonged activation of GOCs, it implies that NMDA channels are located on the GOC dendrites. In this study, a model GOC is represented as a soma and a dendrite whose length is 300 μm (cf. [1]) (Fig. 2). The dendrites of model GOCs are assumed to possess AMPA and NMDA channels. We simulate NMDAR-mediated EPSPs with a double-exponential function with rise and decay time constants of 5 ms and 100 ms, respectively, according to Misra et al. [14].

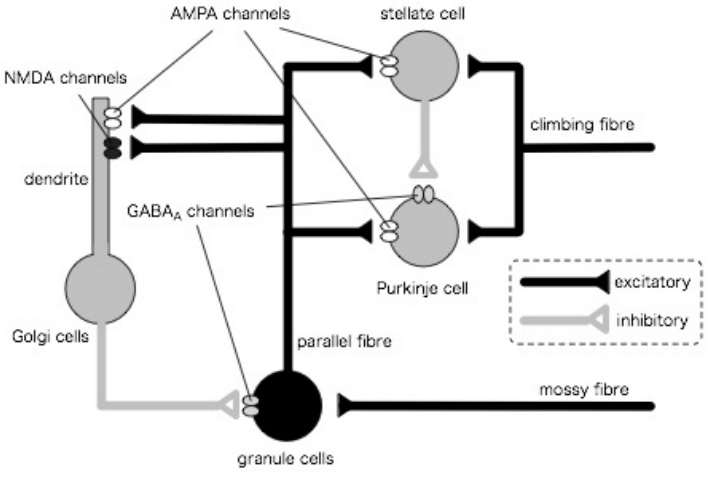

Fig. 2. Grcs' excitation of GOCs is mediated by AMPA and NMDA channels, whereas GOCs' inhibition of GRCs is mediated by $GABA_A$ channels. The strength of current into GRCs, which is induced by MF signal, is external stimulus strength as a control parameter in this model. A PC and an SC are excited by the GRCs mediated by AMPA channels. The PC is inhibited by the SC mediated by $GABA_A$ channels.

2.3 Purkinje and Stellate Cell Models

A PC and an SC are modeled as single-compartment Hodgkin-Huxley units. These cells are assumed to be excited by PF inputs from GRCs mediated by the activation of AMPA channels. The PC is assumed to be inhibited by the SC through $GABA_A$ channels.

2.4 Modeling of a CS

We model MF input signals as current injected directly to the model GRCs, instead of spike trains. Freeman and Muckler [15] have reported that the spontaneous firing rate of MFs is as low as 5 Hz, whereas the firing rate increases up to 30 Hz when stimulated with a tone (e.g. CS). We assume that the current into GRCs increases with the

frequency of firing conveyed through MFs. In simulations, we inject a current I_{MF} of 10.7 pA to all model GRCs for 2 s to simulate GRCs' activities induced by the spontaneous MF activity. For the succeeding 2 s, we inject a current I_{MF} of 29.5 pA to evoke GRCs in response to high frequency MF firing induced by the presentation of the CS. Subsequently, we inject a current I_{MF} of 10.7 pA for 2 s again to resume the baseline activity of GRCs induced by spontaneous MF activity. After conditioning, to simulate network dynamics under CSs of different strengths, we inject current of 31.0 pA or 28.5 pA into GRCs.

2.5 Simulation of Eyeblink Conditioning

For eyeblink conditioning, we present US signal 650 ms after the onset of CS signal presentation. The US signal is sent to both PC and SC. Before conditioning, we set synaptic weights of all PFs at $w_i^{(0)}=1$ and $v_i^{(0)}=1$ for the PC and the SC, respectively. During conditioning, conjunctive stimulation of a CS and a US is assumed to induce LTD and LTP at PF synapses to the PC and the SC, respectively. According to Equations (1) and (2), these synaptic weights are decreased at the PC and increased at the SC when the PFs are activated 50-100 ms before the onset of a US. In addition, we also assume that when spike activity is transmitted to the PC and the SC through PFs alone, PF synapses undergo LTP and LTD, respectively.

$$w_i^{(Tr)} = w_i^{(Tr-1)} 0.9^{f} 1.0005^{f_{tatal}-f}. \tag{1}$$

$$v_i^{(Tr)} = v_i^{(Tr-1)} 1.07^{f} 0.985^{f_{total}-f}. \tag{2}$$

Here, f is the frequency of firing of ith GRC in the interval of 50-100 ms immediately before the onset of a US. f_{tatal} is the total frequency of firing during one trial of conditioning for 2 s. Tr is the trial number. For simplicity, we assume that the US through the climbing fibers affects only learning of PF synaptic weights but not the neurons' activity.

2.6 Data Analysis

When ith GRC $(1 \le i \le N)$ elicits spike activity at time t in response to injected current I^{MF}, $f_i^{(I^{MF})}(t)=1$, and otherwise, $f_i^{(I^{MF})}(t)=0$. We define similarity index (SI) as follows:

$$SI(t_1,t_2) = \frac{\sum_{i=1}^{N} f_i^{I_1^{MF}}(t_1) f_i^{I_2^{MF}}(t_2)}{\sqrt{\sum_{i=1}^{N}\left[f_i^{I_1^{MF}}(t_1)\right]^2}\sqrt{\sum_{i=1}^{N}\left[f_i^{I_2^{MF}}(t_2)\right]^2}}, \tag{3}$$

which represents correlation of a spiking GRC population at time t_1 for CS current I_1^{MF} and that at time t_2 for CS current I_2^{MF}. $SI(t_1,t_2)=1$ indcates that active GRC populations at t_1 and t_2 are identical, where $SI(t_1,t_2)=0$ indicates that completely different GRCs elicit spikes at t_1 and t_2.

3 Results

3.1 POT-Representation

Figure 3*A* represents spike patterns of 20 model GRCs in response to the sustained injection of current of 3 different strengths for simulated CSs. Activation of GRCs by the CS presentation vigorously depolarizes randomly connected GOCs, resulting in the activation of voltage-gated NMDA channels on their dendrites. Because of the long decay time constant of NMDAR-mediated EPSPs, GOCs inhibit nearby GRCs, so that GRCs exhibited random alternations between burst and silent states, as reported by Yamazaki and Tanaka [10].

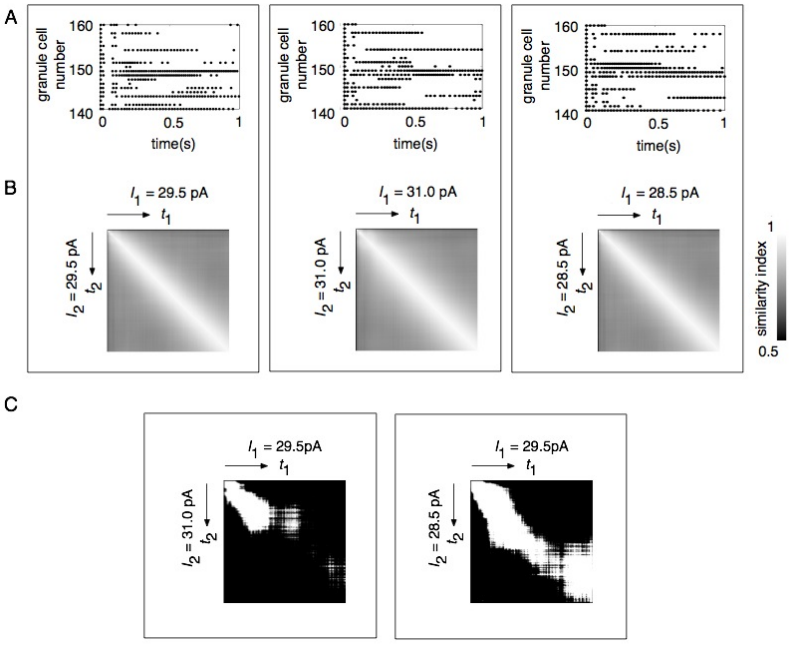

Fig. 3. Network dynamics when current of different strengths is injected to GRCs. (*A*) Spike patterns of 20 GRCs. The abscissa and ordinate represent time and neuron index, respectively. (*B*) *SIs* of spike patterns of GRCs for the same strength of current are plotted in a gray scale between 0.5 and 1. (*C*) *SIs* of spike patterns of GRCs evoked between different strengths of current are plotted in a binary scale in which black (white) indicates $SI \le 0.8$ ($SI > 0.8$).

We show *SIs* of spike patterns of GRCs calculated with Equation 3 in a gray scale (Fig. 3*B*) between 0.5 and 1. Even if the strength of injected current was different, larger *SI* appeared along the diagonal line and gradually decreased with the separation from the diagonal line. This shows that different GRC populations were activated at different times, so that the population of active GRCs changed gradually with time from the CS onset without recurrence. Therefore, the absence of recurrent populations

of active GRCs indicates one-to-one correspondence between a certain population of active GRCs and a certain time, while the sustained current was injected as a CS signal. Thereby, the sequence of active GRC populations is able to represent POT from the CS onset.

3.2 Speeding-Up and Slowing-Down of an Internal Clock

Next, we compared a sequence of GRC populations activated by the sustained injection of current of 29.5 pA with another sequence generated by the injection of current of 31.0pA (28.5 pA). Figure 3*C* shows corresponding SI diagrams. The white band representing high similarity slanted slightly above (below) the diagonal line for the injection of stronger (weaker) current. This indicates that when strong (weak) current is injected, the sequence is compressed (extended). Namely, when input current is stronger (weaker), active GRC populations appear earlier (later) and the speed of generation of active GRC populations becomes faster (slower).

3.3 Simulation of Delay Eyeblink Conditioning

We conducted simulations of delay eyeblink conditioning, in which current injection representing a CS generates a non-recurrent sequence of active GRC populations and a US presented after the CS onset changes synaptic weights of PFs from model GRCs to the model PC and the SC inhibiting the PC.

Before conditioning, the model PC fired at high frequency during the CS presentation (injected current: 29.5 pA). In conditioning, a US signal was given 650 ms after the CS onset. For the model PC, LTD was induced at PF synapses connecting from GRCs active at the timing of the US presentation. For the SC, LTP was induced at PF synapses from those active GRCs.

After 50 trials of conditioning, when we injected current of the same strength as in the conditioning as a CS signal, the PC began to stop firing between 516 ms and 754 ms from the CS onset (Fig. 4*A*). This result indicates that the model PC was able to learn an ISI between CS and US onsets, as consistent with an experiment [16]. On the other hand, when we injected current of 31.0 pA (28.5 pA) as a strong (weak) CS signal, the PC began to stop firing 161ms earlier (898 ms later) than in the default (Fig. 4*B* and *C*). These observations indicate that after conditioning, when a stronger (weaker) CS signal is presented than a CS signal used in conditioning, a PC stopped firing earlier (later). This suggests that even after conditioning, the timing when a CR is elicited can be controlled by the strength of a CS signal.

Next, we examined how the model SC is involved in this timing control after conditioning, by removing the SC after conditioning. First, we injected current of 29.5 pA, the PC began to stop firing between 541 ms and 652 ms after the CS onset (Fig. 4*D*). Although the duration of the PC firing cessation was shorter than that in the default case, the qualitative features of the firing was preserved without the SC. However, when we injected current of 31.0 pA or 28.5 pA after conditioning, the PC kept tonic firing, indicating that the ISI coding was disrupted (Fig. 4*E*, *F*). This suggests that the SC plays an important role for adaptive timing control. Also, when we blocked the plasticity of PF synapses at the SC during conditioning, the PC behaved similarly to the case which a model SC was removed (data not shown).

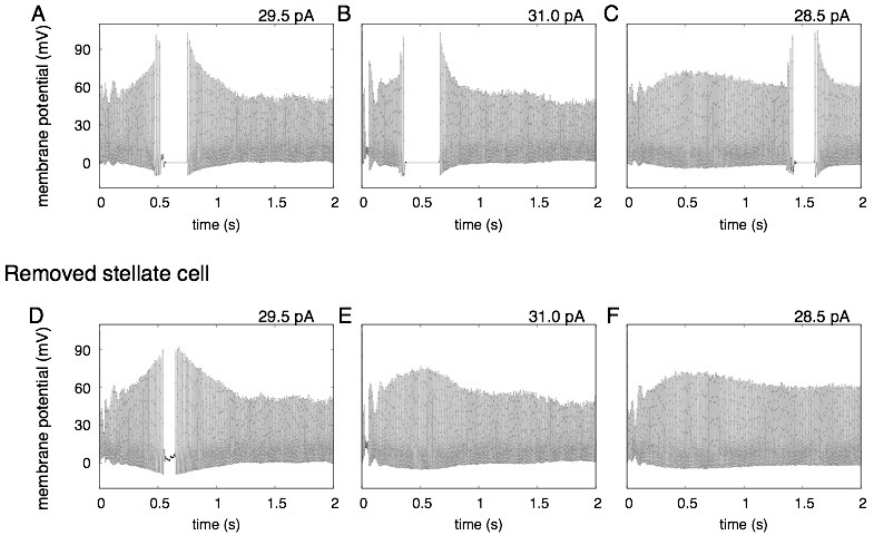

Fig. 4. Membrane potential of the model PC after eyeblink conditioning. In conditioning, US signal is fed to the PC at 650 ms after the onset of sustained injection of current of 29.5 pA to GRCs. (*A*) Membrane potential in response to the current of 29.5 pA after conditioning and (*D*) membrane potential when we remove the SC. (*B*) Membrane potential in response to sustained injection of current of 31.0 pA and (*E*) membrane potential when we remove the SC. (*C*) Membrane potential in response to the current of 28.5 pA and (*F*) membrane potential when we remove the SC. The abscissa represents time from the onset of current injection, and the ordinate represents membrane potential.

4 Discussion and Conclusion

Adaptive control of timing by the strength of external stimulus seems essential for the generalization of motor actions. For example, in batting, we swing a bat at an appropriate timing to hit the ball, estimating the speed of a pitched ball visually. If the speed of a pitched ball is high, we start swinging the bat faster unconsciously. It is expected that the cerebellum learns the timing of motor actions in a supervised manner and controls the learned timing adaptively [17]. In the present study, using our spiking network model of the cerebellar cortex, we argued that a stronger or weaker CS signal conveyed by MFs makes the POT representation change by compressing or expanding the temporal sequence of active GRC populations. Learned timing was advanced or delayed as shown by the temporal shift of timed pause of the PC in the simulated Pavlovian delay eyeblink conditioning, as consistent with experimental findings [18]. We are particularly interested in the role of SCs in the adaptive control of the learned timing. We demonstrated that removing the model SC from the network disrupts the expression of the timing, suggesting that SCs assist the coding of a timing by PCs in motor control, as hypothesized by Rancillac and Crépel [19]. To date, little attention has been paid to the functional role of SCs, except a classical hypothesis as a gain controller of PCs to keep the activity level of PCs within

a physiological range by inhibiting them in a feed-forward manner [20] [21]. The present study shed light for the first time on the functional role of SCs in cerebellar adaptive timing control.

The cerebellum is regarded as a universal simulator that simulates the dynamics of physical and mental objects by acquring the internal models through supervised learning [22] [23]. The present network model of the cerebellar cortex consists of the granular layer that generates a temporal sequence of active GRC populations as liquid states, and a unit composed of a PC and an SC that receives the sequence and extracts time-varying information from the sequence. Once we interpret the granular layer and a PC-SC unit respectively as a reservoir and a readout, our model turns out to be equivalent to a liquid state machine (LSM) [24], a type of artificial neural network model, which is a universal supervised learning machine [25]. In conventional LSMs, a readout is simply a single model neuron that recruits a simple perceptron learning scheme. In contrast, the readout in our model is a pair of two neurons recruiting plasticity of the opposite direction. By this combination, the model cerebellar cortex is able to generalize the timing of a CR adaptively by the strength of a CS signal. This suggests the enhancement of the ability of reading out information from the liquid state in the granular layer. Therefore, the present study may provide insight into the computational power of the cerebellum as a biological counterpart of a liquid state machine. This study also suggests that LSMs can be improved by incorporating inhibitory interneurons in the readout unit.

References

1. Ito, M.: Cerebellum and Neural Control. Raven Press, Hewlett (1984)
2. Yamazaki, T., Tanaka, S.: Neural Modeling of an Internal Clock. Neural Comput. 17, 1032–1058 (2005)
3. Mauk, M.D., Donegan, N.H.: A Model of Pavlovian Eyelid Conditioning Based on the Synaptic Organization of the Cerebellum. Learn. Mem. 3, 130–158 (1997)
4. Hesslow, G., Yeo, C.H.: The Functional Anatomy of Skeletal Conditioning. In: A Neuroscientist's Guide to Classical Conditioning. Springer, New York (2002)
5. Christian, K.M., Thompson, R.F.: Neural Substrates of Eyeblink Conditioning: Acquisition and Retention. Learn. Mem. 11, 427–455 (2003)
6. De Zeeuw, C.I., Yeo, C.H.: Time and Tide in Cerebellar Memory Formation. Curr. Opin. Neurobiol. 15, 667–674 (2005)
7. Maex, R., De Schutter, E.: Synchronization of Golgi and Granule Cell Firing in a Detailed Network Model of the Cerebellar Granule Cell Layer. J. Neurophysiol. 80, 2521–2537 (1998)
8. Palkovits, M., Magyar, P., Szentágothai, J.: Quantitative Histological Analysis of the Cerebellar Cortex in the Cat II Cell Numbers and Densities in the Granular Layer. Brain Res. 32, 13–32 (1971)
9. Mugnaini, E., Atluri, R.L., Houk, J.C.: Fine Structure of Granular Layer in Turtle Cerebellum with Emphasis on Large Glomeruli. J. Neurophysiol. 37, 1–29 (1974)
10. Yamazaki, T., Tanaka, S.: A Spiking Network Model for Passage-of-time Representation in the Cerebellum. Eur. J. Neurosci. 26, 2279–2292 (2007b)
11. Dieudonné, S.: Submillisecond Kinetics and Low Efficacy of Parallel Fibre-Golgi Cell Synaptic Currents in the Rat Cerebellum. J. Physiol. 510, 845–866 (1998)

12. Wong, R.K.S., Stewart, M.: Different Firing Patterns Generated in Dendrites and Somata of CA1 Pyramidal Neurones in Guinea-pig Hippocampus. J. Physiol. 457, 675–687 (1992)
13. Stuart, G.J., Sakmann, B.: Active Propagation of Somatic Action Potentials into Neocortical Pyramidal Cell Dendrites. Nature 367, 69–72 (1994)
14. Misra, C., Brickley, S.G., Farrant, M., Cull-Candy, S.G.: Identification of Subunits Contributing to Synaptic and Extrasynaptic NMDA Receptors in Golgi Cells of the Rat Cerebellum. J. Physiol. 1, 147–162 (2000)
15. Freeman, J.H., Muckler Jr., A.S.: Developmental Changes in Eyeblink Conditioning and Neuronal Activity in the Pontine Nuclei. Learn. Mem. 10, 337–345 (2003)
16. Jirenhed, D., Bengtsson, F., Hesslow, G.: Acquisition, Extinction, and Reacquisition of a Cerebellar Cortical Memory Trace. J. Neurosci. 27, 2493–2502 (2007)
17. Ivry, R.B., Spencer, R.M.: The Neural Representation of Time. Curr. Opin. Neurobiol. 14(2), 225–232 (2004)
18. Svensson, P., Ivarsson, M., Hesslow, G.: Involvement of the Cerebellum in a New Temporal Property of the Conditioned Eyeblink Response. Prog. Brain Res. 124, 317–323 (2000)
19. Rancillac, A., Crépel, F.: Synapses between Parallel Fibres and Dtellate Cells Express Long-term Changes in Synaptic Efficacy in Rat Cerebellum. J. Physiol. 554(Pt. 3), 707–720 (2004)
20. Marr, D.: A Theory of Cerebellar Cortex. J. Physiol. (Lond) 202, 437–470 (1969)
21. Albus, J.S.: A Theory of Cerebellar Function. Math. Biosci. 10, 25–61 (1971)
22. Daniel, M., Wolpert, R., Miall, C., Kawato, M.: Internal Models in the Cerebellum. Trends in Cognitive Sciences 2(9), 338–347 (1998)
23. Ito, M.: Control of Mental Activities by Internal Models in the Cerebellum. Nat. Rev. Neurosci. 9(4), 304–313 (2008)
24. Yamazaki, T., Tanaka, S.: The Cerebellum as a Liquid State Machine. Neural Networks 20(3), 290–297 (2007a)
25. Maass, W., Natschläger, T., Markram, H.: Real-time Computing without Stable States: a New Framework for Neural Computation Based on Perturbations. Neural Comput. 14(11), 2531–2560 (2002)